A Sequential Rotation Array Antenna Comprising Loop Elements With Quasi Two Sources

Kazuhide Hirose, Koki Nishino, Shintaro Mita, and Hisamatsu Nakano

Abstract – Using the method of moments, we analyze two array antennas, each consisting of four radiation elements excited by a *C*-figured feed line and sequentially rotated by 90°. Reference and present antennas have loop elements with a perturbation segment and a branched feed line vertical to the ground plane, respectively. The present antenna exhibits a 3 dB axial ratio bandwidth of 58%, which is wider than the reference antenna by a factor of four. We validate the results by reproducing them using a finite integration technique.

1. Introduction

A loop antenna above the ground plane radiates a circularly polarized (CP) wave [1–5]. The CP radiation is obtained through a loop-shaped deformation [1, 2], an additional segment [3, 4], and quasi two sources using a branched feed line vertical to the ground plane [5]. Recently, the mutual coupling effects between the two loops with quasi two sources have been investigated to expand the 3 dB axial ratio bandwidth threefold compared with an isolated loop [6].

This study is a sequel to the previous one [6] and demonstrates a new development in a loop antenna with quasi two sources. The loop is applied in a sequential rotation array antenna with a *C*-figured feed line for the first time. The radiation characteristics are evaluated using the method of moments (MoM) [7] and compared with those of a sequential array antenna consisting of loops with a perturbation segment.

The technical novelty of this article is optimizing a key parameter for wideband CP radiation, the length (L_C) of a horizontal line connecting the loop to the *C*-figured feed line (see Figure 1). The *C*-figured feed line is characterized by a simple phase shifter and power divider design. This study contributes to the widest axial ratio bandwidth among sequential array antennas [8] using resonant radiation elements excited by a *C*-figured feed line (see Table 1). In Table 1, the unit of an antenna size is the wavelength (scalable configuration), and a scalable configuration is also used in the main text, giving satisfactory performance up to 12 GHz [18]. Note that Table 1 includes studies [15–17] that do not use a *C*-figured feed line for reference.

As mentioned, the widest axial ratio bandwidth is the contribution of this study, which differs from the authors' previous ones [6, 19], as summarized in Table 2. The study [6] discusses a two-element array without a sequential rotation. The study [19] proposes a novel feeding network for a sequential rotation array using a coplanar *O*-figured feed line, not the present multilayer *C*-figured one.

In this study, we first investigate a 3 dB axial ratio bandwidth as a function of length L_C. After optimizing length L_C for a wideband CP wave, we discuss the radiation characteristics, including the gain, voltage standing wave radio (VSWR), and radiation patterns. Finally, the results are compared with those in similar studies.

Manuscript received 16 February 2024.

Kazuhide Hirose, Koki Nishino, and Shintaro Mita are with the College of Engineering, Shibaura Institute of Technology, 3-7-5 Toyosu, Koto, Tokyo 135-8548, Japan; e-mail: khirose@sic.shibaura-it.ac.jp.

Hisamatsu Nakano is with the Science and Engineering, Hosei University, 3-7-2 Kajino, Koganei, Tokyo 184-8548, Japan; e-mail: hymat@hosei.ac.jp.

2. Radiation Characteristics of Present and Reference Antennas

Figures 1a and 1b show configurations and coordinate systems of the present and reference antennas, respectively. Each antenna consists of four square loop elements of perimeter P at a height H above the ground plane. The loop elements are sequentially rotated by 90° and connected to a *C*-figured feed line of radius R via horizontal lines of length L_C. One end of the *C*-figured feed line, point F, is excited using a coaxial line via the vertical line F–F', and the other end T is open circuited.

For the present antenna to radiate a CP wave, the adjacent loop corners of α_n and β_n ($n = 1, 2, 3,$ and 4) are connected to a vertical, branched feed line α_n/β_n–B_n–γ_n, with the bottom end γ_n being connected to a horizontal line of length L_C, as shown in Figure 1a. The branch point B_n is located at height h_B above the ground plane. In contrast, the loop element of the reference antenna has a perturbation segment of length ℓ for CP radiation, and the loop corner β_n is connected to a vertical, straight feed line β_n–γ_n, with the bottom end γ_n being connected to a horizontal line of length L_C, as shown in Figure 1b.

The reason for choosing a loop with a perturbation segment as a reference is that the loop has the axial ratio bandwidth and gain similar to those of the present loop with quasi two sources (and hence was used as a reference loop in the previous study [6]). Note that the perturbation segment plays a role in changing a linearly polarized loop to a CP loop because the current distribution along the loop changes to a traveling wave type [20] from a standing wave type. Also, note that the perturbation segment is located at the center between two adjacent corners, as shown in Figure 1b, for the loop to generate two orthogonal linearly polarized waves necessary for CP radiation. Suppose two adjacent corners of

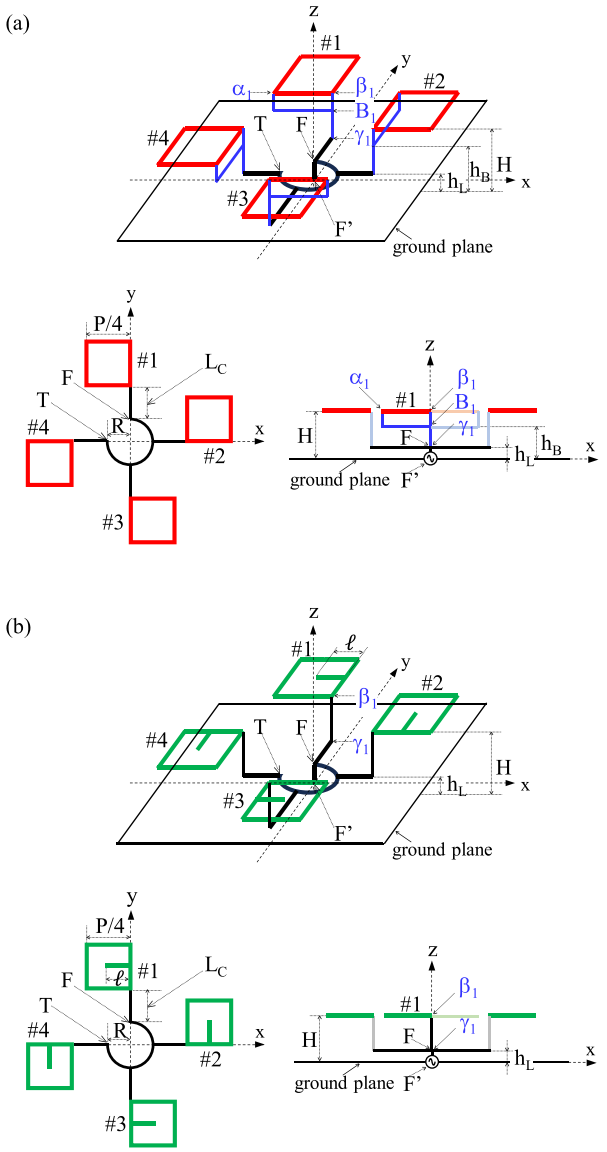

Figure 1. Present and reference antennas consisting of square loops. (a) Present antenna with a branched feedline α_n/β_n–B_n–γ_n (n = 1, 2, 3, and 4) vertical to the ground plane. (b) Reference antenna with a perturbation segment of length ℓ.

a square loop are excited by two sources with the same amplitudes and a phase difference of 90°. In that case, the loop radiates a CP wave, which is also accomplished by quasi two sources [5] using a vertical, branched feed line connected to the two adjacent corners, as shown in Figure 1a.

The horizontal lines and the C-figured feed lines are at a height of h_L for both the present and reference antennas, as shown in Figures 1a and 1b. The antenna is made of wires with a radius ρ [5, 6].

We analyze the antenna using our tailored computer program based on the MoM [7]. The ground plane size is assumed to be infinite, and image theory is used in the analysis. The antenna is designed to radiate a CP wave in the direction normal to the antenna plane in the $+z$-axis direction. We select the loop parameters of (P, h_B, ℓ) and horizontal line length L_C for $R = \lambda_0/(2\pi)$, where λ_0 is the free-space wavelength at a test frequency of f_0. The other configuration parameters are fixed at the same values as those in [5, 6] to facilitate comparison: (H, h_L, ρ) = ($\lambda_0/4$, $\lambda_0/50$, $\lambda_0/200$). Note that the C-figured feed line has a path length of $\lambda_0/4$ between its branches for an excitation phase difference of 90°.

The horizontal line length L_C of the present antenna is a crucial parameter for wideband CP radiation because a variation in L_C controls the amount of the mutual coupling between the loop elements. The mutual coupling effects between the two loops with quasi two sources expand the axial ratio bandwidth threefold compared with an isolated loop [6].

The simulated 3 dB axial ratio bandwidth versus L_C is shown with a solid line in Figure 2. At each value of L_C, the loop parameters (P, h_B) are selected for the axial ratio bandwidth to become a maximal value. For comparison, the dotted line shows the result of the reference antenna, where the loop parameters (P, ℓ) are selected, each with a value of L_C. The present antenna's bandwidth has a peak value of 58%, whereas the reference one remains almost unchanged at 14%. We can say that the present antenna has a wider bandwidth than the reference antenna by a factor of four (=58/14).

A question arises when looking at the axial ratio bandwidth of the present antenna in Figure 2. Why does the bandwidth increase with an increase in the

Table 1. Comparison with similar studies[a]

Study	Array type	Radiation element	ARBW (%)	Gain (dBi)	Operating frequency (GHz)	Antenna size $x \times y \times z$ (λ_0^3) (z: height)
[9]	2 × 2	Patch	8.3	10.8	8.25	1.3 × 1.3 × 0.04
[10]	2 × 2	Patch	15	–	5.3	1.3 × 1.4 × 0.58
[11]	2 × 2	Patch	20.4	11.1	27	2.9 × 2.9 × 0.10
[12]	2 × 2	Patch	15.2	–	60	1.8 × 1.8 × 0.05
[13]	2 × 2	Loop	30	11.9	3	1.4 × 1.4 × 0.25
This study	2 × 2	Loop	49	11.6	3	1.1 × 1.1 × 0.25
[14]	2 × 2	Patch	15.5	8.25	5.75	0.9 × 0.9 × 0.03
[15]	2 × 2	Dipole	21.9	12.4	21	– × – × 0.14
[16]	2 × 2	Patch	20.2	13.8	28	1.5 × 1.5 × 0.07
[17]	2 × 2	Patch	23.9	14.6	64	2.1 × 4.2 × 0.50

[a] ARBW, 3 dB axial ratio bandwidth; –, not described.

Table 2. Comparison to authors' previous studies

Study	Array type	Radiation element	Sequential rotation	Feeding network	Contribution
[6]	1×2	Loop	Not applied	Multilayer Straight	Novel dual-wire antenna
[19]	2×2	Spiral	Applied	Coplanar *O* figured	Novel feeding network for sequential rotation array
This study	2×2	Loop	Applied	Multilayer *C* figured	Widest ARBW[a] among resonant element array

[a] ARBW: 3 dB axial ratio bandwidth.

horizontal line length L_C and start decreasing after some limit at $L_C \approx 0.15\lambda_0$? To answer this question, we refer to the previous study [6], where the bandwidth of an array of two square loop antennas with quasi two sources is investigated as a function of the distance d between the antennas, as shown in Figure 3a. The result is shown with a solid line in Figure 3c. The bandwidth increases with an increase in d and starts decreasing after some limit at $d \approx 0.15\lambda_0$, as the bandwidth behavior of the present antenna. In summary, the bandwidth behavior versus L_C for the present antenna can be explained using the mutual coupling between two loop antennas with quasi two sources. Note that a dotted line in Figure 3c also shows the result of an array of two square loop antennas with a perturbation segment shown in Figure 3b. The bandwidth remains unchanged with an increase in the distance d between the antennas, which does not conflict with the result of the reference antenna (see the dotted line in Figure 2).

The solid lines in the lower part of Figure 4 show the simulated gain and axial ratio versus frequency for the present antenna. The horizontal line length is $L_C = 0.13\lambda_0$ with $(P, h_B) = (1.04\lambda_0, 0.10\lambda_0)$. The gain has a maximum value of 11.7 dBi and drops from the maximum one by 3 dB at $1.30f_0$ in the axial ratio bandwidth. When considering this, the overlapped bandwidth is 51% ($0.77f_0$ to $1.30f_0$). For comparison, the dotted lines show the results of the reference antenna for $L_C = 0.13\lambda_0$ with $(P, \ell) = (1.11\lambda_0, 0.27\lambda_0)$. The axial ratio bandwidth is 14%, where the gain is more than 7.8 dBi, with a maximum value of 7.9 dBi. Note that the reference and present antennas have the dimensions summarized in Table 3.

A solid line in the upper part of Figure 4 shows the simulated VSWR of the present antenna. The VSWR is evaluated for a 75 Ω coaxial line. The present antenna exhibits a VSWR of less than two in a frequency range of $0.74f_0$ to $1.27f_0$. Taking this into consideration, we evaluate a bandwidth of 49% ($0.77f_0$ to $1.27f_0$), where the axial ratio and VSWR determine the lower and upper frequency edges, respectively.

Figures 5a and 5b show the radiation patterns of the present and reference antennas, respectively. The pattern is illustrated with dotted and solid lines showing right-hand (E_R) and left-hand (E_L) CP wave components, respectively. The present antenna shows lower cross-polarized radiation than the reference one. In addition, the present antenna's half-power beamwidth (HPBW) is narrower than the reference antenna's. Average HPBWs in the $\phi = 0°$ and 90° planes are 46° and 58° for the present and reference antennas, respectively. The gain of the present antenna is 11.6 dBi, higher than the reference antenna by 3.8 dB.

It is necessary to explain how the HPBW of the present antenna significantly improves compared with the reference antenna. Further calculations reveal that

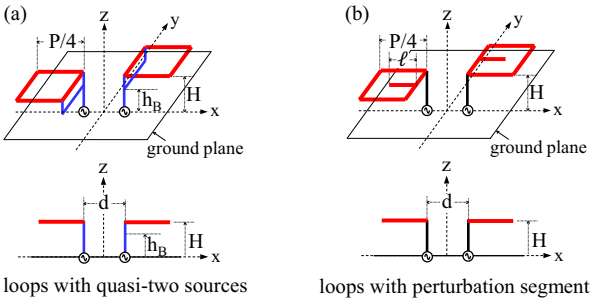

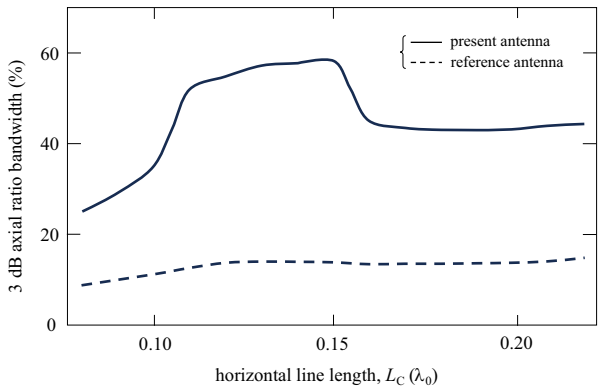

Figure 2. Simulated 3 dB axial ratio bandwidth versus horizontal line length L_C.

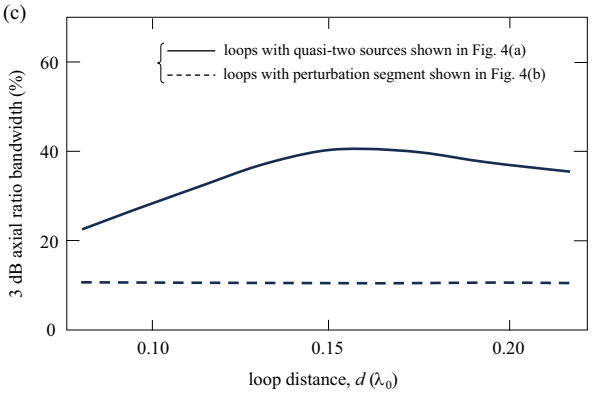

Figure 3. Simulated 3 dB axial ratio bandwidth versus distance between two loop antennas [6].

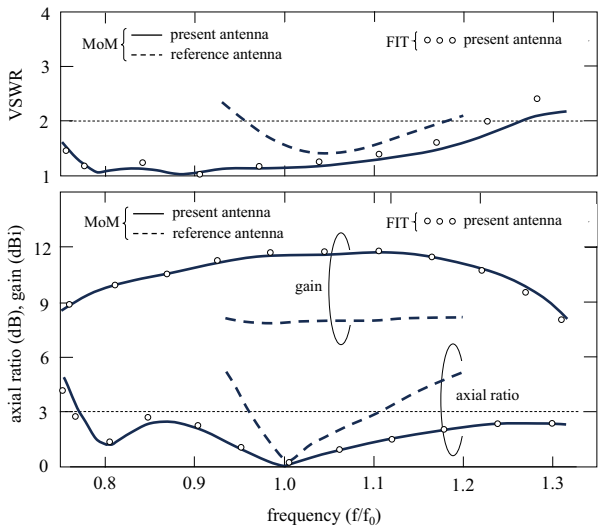

Figure 4. Simulated gain, axial ratio, and VSWR versus frequency.

Table 3. Dimensions of present and reference antennas designed

		Antenna	
Antenna part	Parameter	Present	Reference
Loop	Perimeter P (λ_0)	1.04	1.11
	Branch height h_B (λ_0)	0.10	Not applied
	Perturbation segment length $\ell(\lambda_0)$	Not applied	0.27
	Height H (λ_0)	1/4	
Feed line	Horizontal line length L_C (λ_0)	0.13	
	C-figured feed line radius R (λ_0)	$1/(2\pi)$	
	Height h_L (λ_0)	1/50	
All	Wire radius ρ (λ_0)	1/200	

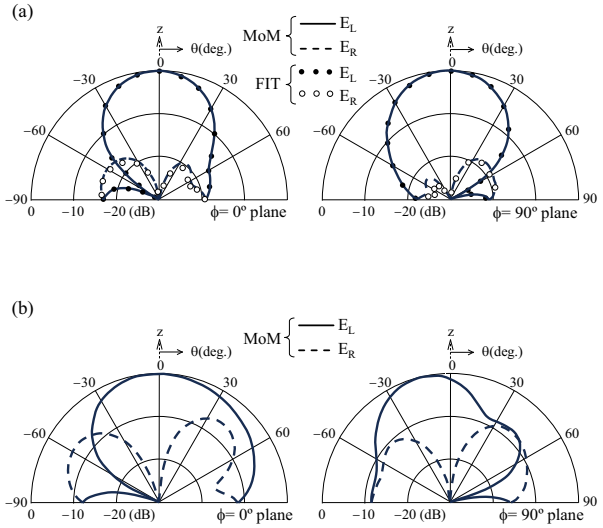

Figure 5. Simulated radiation patterns. (a) Present antenna. (b) Reference antenna.

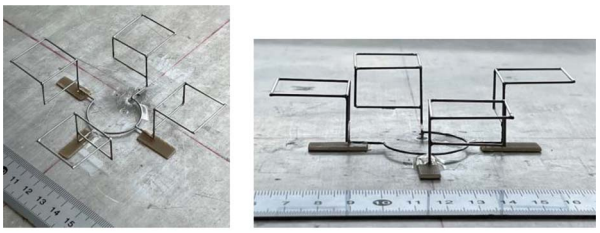

Figure 6. Photographs of a prototype. (a) Perspective view. (b) Side view.

the average HPBW of the reference antenna improves (to 43°), as the horizontal line length further increases (to $L_C = 0.25\lambda_0$). This means that a line length of $L_C = 0.13\lambda_0$ is too small for the reference antenna to exhibit a satisfactory HPBW. Therefore, it can be said that the mutual coupling effects of the present antenna also contribute to an improvement in the HPBW.

To validate the results using the MoM, we reproduce them using an EM simulation solver on a finite integration technique (FIT) [21]. Small circles and dots in Figures 4 and 5a are the results using the FIT. They agree well with the MoM results.

Finally, we compare our results with those in similar studies using resonant radiation elements excited by a

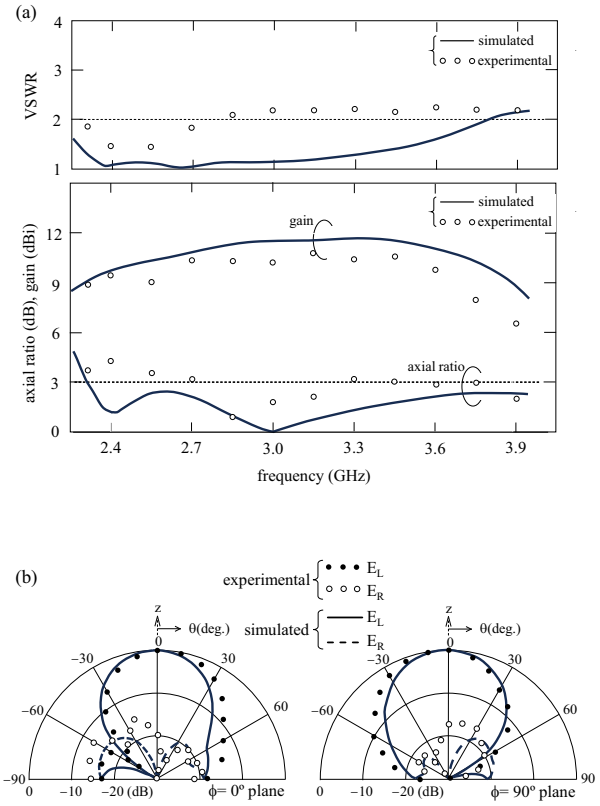

Figure 7. Experimental and simulated results of the present antenna. (a) Frequency responses of gain, axial ratio, and VSWR. (b) Radiation patterns. Note that the simulated results are identical to those with the MoM in Figures 4 and 5a.

C-figured feed line. The comparisons are summarized in Table 1. The present antenna has the widest axial ratio bandwidth.

As additional data, we show photographs of an antenna fabricated at $f_0 = 3.0$ GHz and tentative experimental results in Figures 6 and 7, respectively. The experimental results are similar to the MoM results that are identical to those in Figures 4 and 5a.

3. Conclusions

We have studied present and reference array antennas consisting of loops with quasi two sources and a perturbation segment, respectively. The loops are excited by a *C*-figured feed line via horizontal lines of length L_C. As the length L_C is varied, the 3 dB axial ratio bandwidth of the present antenna reaches 58%, whereas the bandwidth of the reference antenna remains almost unchanged at 14%. To validate the results using the MoM, we reproduce them using a FIT. The antenna has an overlapped bandwidth of 49%, where the axial ratio and VSWR are less than 3 dB and 2, respectively.

4. Acknowledgment

The authors thank Blair Thomson for invaluable assistance in preparing this manuscript.

5. References

1. Y. Murakami, T. Nakamura, A. Yoshida, and K. Ieda, "Rectangular Loop Antenna for Circular Polarization," *Transactions IEICE*, **J78-B-II**, 7, July 1995, pp. 520-527.
2. Y. Zhang and L. Zhu, "Printed Dual Spiral-Loop Wire Antennas for Broadband Circular Polarization," *IEEE Transactions on Antennas and Propagation*, **54**, 1, January 2006, pp. 284-288.
3. H. Nakano, "A Numerical Approach to Line Antennas Printed on Dielectric Materials," *Computer Physics Communications*, **68**, 1–3, November 1991, pp. 441-450.
4. T. Han, C. Sim, and C. Chen, "A Circularly Polarized Meander Loop Antenna Design for GNSS Application," *IEEE Antennas and Wireless Propagation Letters*, **20**, 12, December 2021, pp. 2235-2239.
5. K. Hirose, S. Tsubouchi, and H. Nakano, "A Loop Antenna with Quasi-Two Sources for Circular Polarisation," *Electronics Letters*, **58**, 6, January 2022, pp. 222-224.
6. K. Hirose, K. Nishino, and H. Nakano, "Dual-Loop Antennas With an Expanded Axial Ratio Bandwidth," *Electronics Letters*, **59**, 8, April 2023, p. e12784.
7. R. F. Harrington, *Fields Computation by Moment Methods*, New York, Macmillan, 1968.
8. H. Nakano, S. Matsumoto, and N. Ochiai, "Improvement of the Axial Ratio for Circularly Polarized Multi-Arm Antenna," *Proceedings of the Combined Conference of Four Institutions Related to Electrical Engineering in Japan*, 1975, p. B-21.
9. D. Hester, S. Han, and M. Adams, "Design Methodology for Single-Feed Circularly Polarized X-Band Antenna Arrays for CubeSats Using Multilevel Sequential Rotation," *IEEE Journal on Miniaturization for Air and Space Systems*, **5**, 1, March 2024, pp. 42-50.
10. C. E. Santosa, J. Sumantyo, S. Gao, and K. Ito, "Broadband Circularly Polarized Microstrip Array Antenna With Curved-Truncation and Circle-Slotted Parasitic," *IEEE Transactions on Antennas and Propagation*, **69**, 9, September 2021, pp. 5524-5533.
11. M. Sun, N. Liu, L. Zhu, and G. Fu, "Wideband Circularly Polarized Sequentially Rotated Microstrip Antenna Array With Sequential-Phase Feeding Network," *Journal of Communications and Information Networks*, **5**, 3, September 2020, pp. 350-357.
12. B. Lee and Y. Yoon, "Low-Profile, Low-Cost, Broadband Millimeter-Wave Antenna Array for High-Data-Rate WPAN Systems," *IEEE Antennas and Wireless Propagation Letters*, **16**, April 2017, pp. 1957-1960.
13. K. Hirose, Y. Kikkawa, S. Tsubouchi, and H. Nakano, "Fundamental Study on Comb-Line Antennas Modified With Loop Elements for Increased Axial Ratio Bandwidth," *Progress in Electromagnetics Research M*, **115**, February 2023, pp. 59-69.
14. S. Maddio, "A Compact Wideband Circularly Polarized Antenna Array for C-Band Application," *IEEE Antennas and Wireless Propagation Letters*, **14**, January 2015, pp. 1081-1084.
15. W. Zeng, X. Wu, F. Wu, Y. Zang, Z. Jiang, et al., "Broadband Dual-CP Multi-Stage Sequential Rotation Arrays With Independent Control of Polarizations Based on Dual-CP Magneto-Electric Dipole Elements," *IEEE Transactions on Antennas and Propagation*, **72**, 4, April 2024, pp. 3017-3032.
16. P. PourMohammadi, P. Fei, H. Nasseri, Q. Zheng, O. Babarinde, et al., "A Single-Layer Compact Wideband Circularly Polarized Patch Array for 5G Communications," *IEEE Antennas and Wireless Propagation Letters*, **22**, 4, April 2023, pp. 754-758.
17. Z. Qi, Y. Zhu, and X. Li, "Compact Wideband Circularly Polarized Patch Antenna Array Using Self-Sequential Rotation Technology," *IEEE Antennas and Wireless Propagation Letters*, **21**, 4, April 2022, pp. 700-704.
18. H. Nakano, T. Oka, K. Hirose, and J. Yamauchi, "Analysis and Measurements for Improved Crank-Line Antennas," *IEEE Transactions on Antennas and Propagation*, **45**, 7, July 1997, pp. 1166-1172.
19. K. Hirose, N. Ito, Y. Urushibata, and H. Nakano, "A Novel Feeding Network for Sequential Rotation Array Antennas Above the Ground Plane," *URSI Radio Science Letters*, **5**, January, 2024, pp. 1-5.
20. K. Hirose, M. Nakatsu, and H. Nakano, "A Loop Antenna With Enlarged Bandwidth of Circular Polarization—Its Application in a Comb-Line Antenna," *Progress in Electromagnetics Research C*, **105**, September 2020, pp. 175-184.
21. CST Studio Suite, https://www.cst.com/applications/mwandrf (Accessed 24 January 2024).